UDC 621.396+621.3.093.2

COMBINED INFLUENCE OF DOPPLER EFFECT AND PILOT DE-ORTHOGONALIZATION ON 2×2 TO 4×4 MIMO SYSTEMS AND IMPROVEMENT OF ORTHOGONAL SEQUENCES

Romanuke V. V.

O. S. Popov Odesa National Academy of Telecommunications,
1 Kuznechna St., Odesa, 65029, Ukraine.
romanukevadimv@gmail.com

КОМБІНОВАНИЙ ВПЛИВ ЕФЕКТУ ДОПЛЕРА І ПІЛОТНОЇ ДЕОРТОГОНАЛІЗАЦІЇ НА MIMO-СИСТЕМИ ВІД 2×2 ДО 4×4 ТА ПОКРАЩЕННЯ ОРТОГОНАЛЬНИХ ПОСЛІДОВНОСТЕЙ

Романюк В. В.

Одеська національна академія зв'язку ім. О. С. Попова,
65029, Україна, м. Одеса, вул. Кузнечна, 1.
romanukevadimv@gmail.com

КОМБИНИРОВАННОЕ ВЛИЯНИЕ ЭФФЕКТА ДОПЛЕРА И ПИЛОТНОЙ ДЕОРТОГОНАЛИЗАЦИИ НА MIMO-СИСТЕМЫ ОТ 2×2 ДО 4×4 И УЛУЧШЕНИЕ ОРТОГОНАЛЬНЫХ ПОСЛЕДОВАТЕЛЬНОСТЕЙ

Романюк В. В.

Одесская национальная академия связи им. А. С. Попова,
65029, Украина, г. Одесса, ул. Кузнечная, 1.
romanukevadimv@gmail.com

Abstract. The Doppler effect in 2×2, 3×3, and 4×4 MIMO wireless communication systems with channel state estimation is studied. The orthogonal pilot signal approach is used for the channel estimation, where the Hadamard sequences are used for piloting along with the eight Romanuke orthogonal sets similar to the Walsh set. The Doppler effect is additionally aggravated by the pilot signal de-orthogonalization, where two negative-to-positive symbol errors are assumed to have occurred while signal is transmitted. MIMO transmissions are simulated for 10 cases of the frame length and pilot symbols per frame by no Doppler shift to 1100 Hz Doppler shift with a step of 100 Hz. By assuming that the carrier frequency is 5,9 GHz, the step corresponds to a motion speed of about 18.3 km/hr. Based on the simulations, it is ascertained that the Doppler effect negatively influences transmissions of long data packets. It is impracticable to apply MIMO transmissions of long packets at speeds exceeding 100 km/hr. To maintain an appropriate MIMO link data rate, the packet length should be shortened as the motion speed increases. On the other hand, the MIMO performance is substantially improved by increasing the number of antennas, except for the case of transmitting long packets. Besides, under the de-orthogonalization caused by two negative-to-positive symbol errors, the MIMO Walsh pilot sequences are outperformed by MIMO Romanuke pilot sequences, so the latter are considered as an improvement of MIMO orthogonal sequences. However, the performance difference between the Romanuke and Walsh pilot sequences decays as a greater number of transmit-receive antenna pairs is used and the motion speed increases.

Key words: wireless communication system; MIMO; channel state estimation; orthogonal pilot signal approach; Walsh binary functions; Romanuke binary functions; Doppler effect; de-orthogonalization.

Анотація. Вивчається ефект Доплера у системах безпровідної комунікації MIMO від 2×2 до 4×4 з оцінюванням стану каналів. Для оцінювання каналів застосовується підхід ортогональних пілотуючих сигналів, де для пілотування використовуються послідовності Адамара разом з вісьмома ортогональними наборами автора, котрі є подібними до набору Уолша. Ефект Доплера додатково загострений деортогоналізацією пілотуючих сигналів, де припускається, що під час передачі сигналу виникли дві помилки символів типу перескоку від від'ємного до додатного значення. MIMO-передачі симулюються для 10 випадків довжини блока даних та пілотуючих символів у блоці, починаючи від випадку відсутності доплерівського зсуву до випадку доплерівського зсуву в 1100 Гц з кроком у 100 Гц. Припускаючи, що частотою носійної є 5,9 ГГц, цей крок відповідає швидкості близько 18,3 км/год. Ґрунтуючись на симуляціях, встановлюється, що ефект Доплера негативно впливає на передачі довгих пакетів даних. Застосування MIMO-передач довгих пакетів є недоцільним на швидкостях, що перевищують 100 км/год. Для того, щоб підтримувати прийнятну швидкість передачі даних у MIMO-з'єднаннях, довжина пакетів зі збільшенням швидкості переміщень повинна скорочуватись. З іншого боку, продуктивність MIMO суттєво покращується, за виключенням випадку передавання довгих пакетів, при збільшенні кількості антен. Крім того, при деортогоналізації послідовності Уолша програють у продуктивності послідовностям автора, так що останні розглядаються як покращення ортогональних послідовностей MIMO. Проте різниця у продуктивності між пілотуючими послідовностями автора й Уолша згасає з використанням більшої кількості передавально-приймальних антен та зростанням швидкості пересування.

Ключові слова: система безпровідної комунікації; MIMO; оцінювання стану каналів; підхід ортогональних пілотуючих сигналів; бінарні функції Уолша; бінарні функції автора; ефект Доплера; деортогоналізація.

Аннотация. Изучается эффект Доплера в системах беспроводной коммуникации MIMO от 2×2 до 4×4 с оцениванием состояния каналов. Для оценивания каналов применяется подход ортогональных пилотирующих сигналов, где для пилотирования используются последовательности Адамара вместе с восемью ортогональными наборами автора, являющиеся подобными набору Уолша. Эффект Доплера дополнительно обострён деортогонализацией пилотирующих сигналов, где предполагается, что во время передачи сигнала произошли две ошибки символов типа перескока от отрицательного к положительному значению. MIMO-передачи симулируются для 10 случаев длины блока данных и пилотирующих символов в блоке, начиная от случая отсутствия доплеровского сдвига до случая доплеровского сдвига в 1100 Гц с шагом 100 Гц. Предполагая, что частота несущей равна 5,9 ГГц, этот шаг соответствует скорости приблизительно 18,3 км/ч. Основываясь на симуляциях, устанавливается, что эффект Доплера негативно влияет на передачи длинных пакетов данных. Применение MIMO-передач длинных пакетов нецелесообразно на скоростях, превышающих 100 км/ч. Для того, чтобы поддерживать приемлемую скорость передачи данных в MIMO-соединениях, длина пакетов с увеличением скорости передвижений должна сокращаться. С другой стороны, производительность MIMO существенно улучшается, за исключением случая передачи длинных пакетов, при увеличении количества антенн. Кроме того, при деортогонализации последовательности Уолша проигрывают в производительности последовательностям автора, так что последние рассматриваются как улучшение ортогональных последовательностей MIMO. Однако разность в производительности между пилотирующими последовательностями автора и Уолша угасает с использованием большего количества антенн и возрастанием скорости передвижений.

Ключевые слова: система беспроводной коммуникации; MIMO; оценивание состояния каналов; подход ортогональных пилотирующих сигналов; бинарные функции Уолша; бинарные функции автора; эффект Доплера; деортогонализация.

Orthogonal piloting and de-orthogonalization in MIMO. Currently, information exchange is very intensive owing to using wireless communication technologies. In Ukraine, as of 2020, the 5G wireless communication technology is the most promising and is still being tested before becoming eventually widespread. For multiplying the capacity of a radio link by using multiple antennas at the transmitter and receiver ends, 5G networks use the MIMO technique and massive MIMO approach [1]. It is well known that, due to the Doppler effect, the quality of wireless communication may dramatically worsen when either or both the transmitter and receiver end is in motion [2, 3]. However, the influence of Doppler shifts on the MIMO performance at human-walking speeds is negligible. Nonetheless, at vehicular speeds the influence is experienced to be more significant, especially when the vehicle makes accelerations [3, 4]. To sustain high quality of links under Doppler shifts and combined effects of scattering, fading, and power decay with distance, MIMO operates, in particular, on channel state information (CSI) [1, 5, 6]. The CSI is extracted from the received signal by using orthogonal pilot signals prepended to every packet [7]. Thus, the orthogonal pilot signal approach (OPSA) for channel state estimation (CSE) has a higher overhead, but it achieves a better channel estimation accuracy than without any known transmitted sequence [8].

Obviously, longer orthogonal pilot sequences are expected to ensure better MIMO performance. Nevertheless, it is very important to remember that orthogonal pilot sequences cannot be too long as well. In practice, the length of orthogonal pilot sequences is limited by the coherence time of the channel [4]. Besides, the reuse of pilot sequences of several co-channel cells leads to pilot contamination that worsens the MIMO performance [9]. Another problem is that a loss of a symbol (this is, in other words, a symbol error) in a pilot sequence leads to the pilot signal de-orthogonalization. The pilot signal de-orthogonalization occurs due to channel noise and interference. Obviously, the pilot signal de-orthogonalization may additionally worsen the MIMO performance.

The orthogonality in MIMO is based on Walsh functions [10] generated from the Hadamard matrix [11]. This is done as well in other wireless communication systems exploiting orthogonality [1, 4, 11, 12]. In MIMO, the first orthogonal sequence of pilot symbols is usually the sequence of ones, which is the Walsh function of the zeroth order (being a function-constant) [10]. The second orthogonal sequence of pilot symbols, in the given finite binary basis ordered by Walsh [10, 11], is the Walsh function of the last order. This function is an ideal meander of the highest frequency [11]. Considering Walsh functions from the middle of the unit interval on which they are defined, the structure of Walsh functions is symmetrical [10, 11, 13]. Partially unsymmetrical binary functions which constitute orthogonal bases are known also (e. g., see [11, 13, 14]). The eight orthogonal bases of such unsymmetrically-structured binary functions (considering the seven non-zeroth-order functions in every basis; the function-constant, which is the zeroth-order function in every basis, is not considered) found by Romanuke [11] were simulated to substitute the respective Walsh functions in wireless communication systems with the code division multiple access [15, 16]. It was shown in [11] and [14] that these orthogonal sets of binary functions outperform a Walsh set, where the bit-error rate (BER) is decreased by 3 to 5 %. Thus, it is thereafter assumed that BER in MIMO systems with OPSA affected by both the Doppler effect and pilot signal de-orthogonalization might be decreased by using the similar substitution. This is believed to increase general throughput and reliability of MIMO links.

The goal and tasks to achieve it. The goal is to estimate the BER performance of 2×2, 3×3, and 4×4 MIMO systems with CSE by the OPSA for both the Walsh (Hadamard) and Romanuke binary functions for a wide range of Doppler shifts by the pilot signal de-orthogonalization. For this, various relationships of the frame length and pilot symbols per frame will be considered by when the negative value of a binary function at a random place is switched into the positive value. Such a switching (implying a symbol error) is assumed to have occurred twice within a definite set of orthogonal pilot sequences used for CSE. The estimated BER performance is believed to answer the question on MIMO efficiency by ascertaining whether increasing the number of antennas mitigates the Doppler effect aggravated by the pilot signal de-orthogonalization. A possibility of CSE by the OPSA by more appropriate orthogonal sets is to be studied as well.

To achieve the goal, 2×2 to 4×4 MIMO wireless communication systems with CSE will be simulated, where the number of transmit and receive antennas is the same (two, three, and four, respectively). The simulation will be configured and carried out by using MATLAB® R2019a Communications System Toolbox™ (CST) functions. The BER performance is to be plotted versus a ratio of bit energy to noise power spectral density. The range of the bit-energy-to-noise-density ratio (BENDR) is set from 0 dB to 8 dB with a step of 1 dB. The range of Doppler shifts is from zero to a value at which the moving object (implying the vehicle itself or a motion of antennas) achieves express train speeds or so.

Simulation parameters and set-up. While the modulated signal is encoded, the symbol rate of the code is 1 for a 2×2 MIMO system, and is 3/4 for 3×3 and 4×4 MIMO systems. To match the symbol rate with piloting, the frame length denoted by F is set at 36, 72, 144, 288 symbols. Subsequently, the number of pilot symbols per frame denoted by P, which commonly does not exceed 25 % of the frame length, is set at integers shown in Table 1, with respect to each frame length. This results in the 10 subcases of the two parameters paired for simulation.

Table 1 – The 10 subcases of the frame length and number of pilot symbols per frame

P	8	16	32	64	8	16	32	8	16	8
F	288	288	288	288	144	144	144	72	72	36

In an $N \times N$ MIMO system, the N pilot sequences are taken as the first N Walsh Hadamard-ordered functions from the basis of P functions (see an example in Fig. 1). In the case of using orthogonal codes by Romanuke functions [11], the N pilot sequences are taken as the last N binary functions from each of the eight bases of P functions (see an example in Fig. 2).

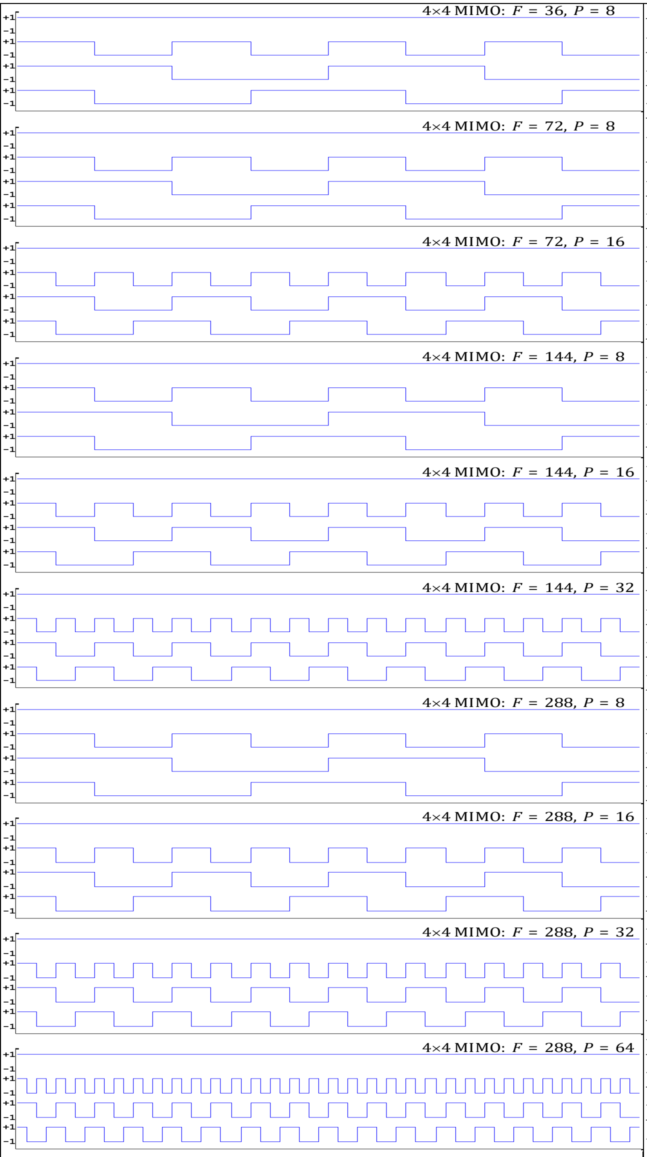

Figure 1 – The four Walsh Hadamard-ordered orthogonal functions in a 4×4 MIMO system

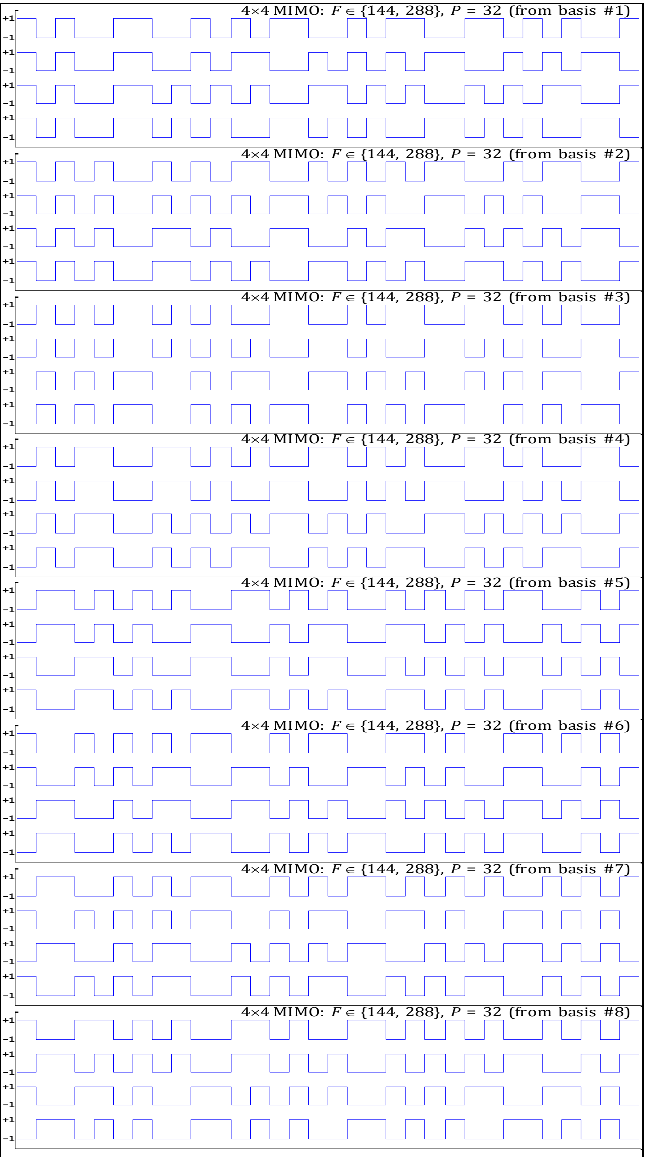

Figure 2 – The four last Romanuke binary functions in a 4×4 MIMO system

In the CST simulation, the data are modulated and encoded as follows. For using 2 to 4 transmit antennas, the signal is modulated by applying the quaternary phase shift keying (QPSK) method. This is realized by the QPSKModulator object. The modulated signal is then encoded by using the OSTBCEncoder object. The OSTBCEncoder object encodes an input symbol sequence using orthogonal space-time block code (OSTBC). The block maps the input symbols block-wise and concatenates the output codeword matrices in the time domain.

For each of those 9 BENDR points (from 0 dB to 8 dB with a step of 1 dB), maximum 50,000 packets are transmitted through flat-fading Rayleigh channels [17], to which white Gaussian noise is added by applying the CST AWGNChannel object. It is assumed that the channel remains unchanged for the length of the packet (i. e., it undergoes slow fading). Besides, it is additionally assumed that the channel undergoes independent fading between the multiple transmit-receive antenna pairs [18].

At the receiving end, the signal is combined and demodulated. For this, the CST OSTBCCombiner object combines the signals from all of the receive antennas and the channel estimate signal to extract the soft information of the symbols encoded by an OSTBC. The combining algorithm uses only the estimate for the first symbol period per codeword block. The output of the combiner is demodulated by applying the CST QPSKDemodulator object. While an end-to-end MIMO system is simulated, the number of errors is registered for every BENDR point at each Doppler shift (including no motion, i. e. by zero Doppler shift) for every subcase in Table 1.

The maximum number of errors is 10 % of the maximum number of packets. So, if 5,000 errors occur at a given BENDR, the simulation loop for the given BENDR is broken.

Denote the speed of the motion (of either a moving vehicle itself or antennas) by $\tilde{v}$. Denote the Doppler shift measured in Hz by S_{Doppler}. If f_{carrier} is the carrier frequency in GHz, then speed $\tilde{v}$ measured in km/hr is expressed via S_{Doppler} and f_{carrier} as

$$\tilde{v} = \frac{1.08 \cdot S_{\text{Doppler}}}{f_{\text{carrier}}} . \quad (1)$$

So, lesser carrier frequencies correspond to faster motion. By assuming that the carrier frequency is 5,9 GHz, speed $\tilde{v}$ is approximately estimated by (1) as

$$\tilde{v} = 0.18305 \cdot S_{\text{Doppler}} . \quad (2)$$

Relationship (2) will be further used for interpreting various Doppler shifts, i. e. for translating them into understandable speeds in order to compare and discuss possible motion limitations (if any) for the sake of maintaining reasonable MIMO performance.

Visualization of the simulation results. To begin, it is necessary to have a benchmark. For this, the BER performance versus BENDR by no motion is plotted in Fig. 3, where Hadamard sequences are marked with squared points and the Romanuke orthogonal sequences are marked with circled points. The polylines for a MIMO system with a greater number of transmit-receive antenna pairs are visualized thicker. The same markers and line thickness will be used further. Fig. 3 shows that the polylines for 2×2 MIMO systems are above the polylines for 3×3 MIMO systems, and the latter are above the polylines for 4×4 MIMO systems, i. e. the best performance by no motion is achieved by increasing the number of transmit-receive antenna pairs. It is also seen that the least BER is obtained by transmitting longer packets with long pilot sequences. In particular, these are subcases of $F = 288$ by $P = 32$ and $P = 64$.

According to relationship (2), an approximate motion speed at a 100 Hz Doppler shift is about 18.3 km/hr. The BER performance for this case (Fig. 4) is very similar to that in Fig. 3. Moreover, the BER performance at a 200 Hz Doppler shift (Fig. 5) appears to be similar to them as well. The case of urban speeds (Fig. 6) does not differ much from these cases of relatively slow motion. Indeed, the polylines for the subcases of $\{F = 144, P = 32\}$ and $F = 288$ by $P = 32$ and $P = 64$ are still stuck together, whereas the others are disjoined. A noticeable deterioration of the performance is seen in Fig. 7. At highway speeds (Fig. 8), the BER worsens significantly.

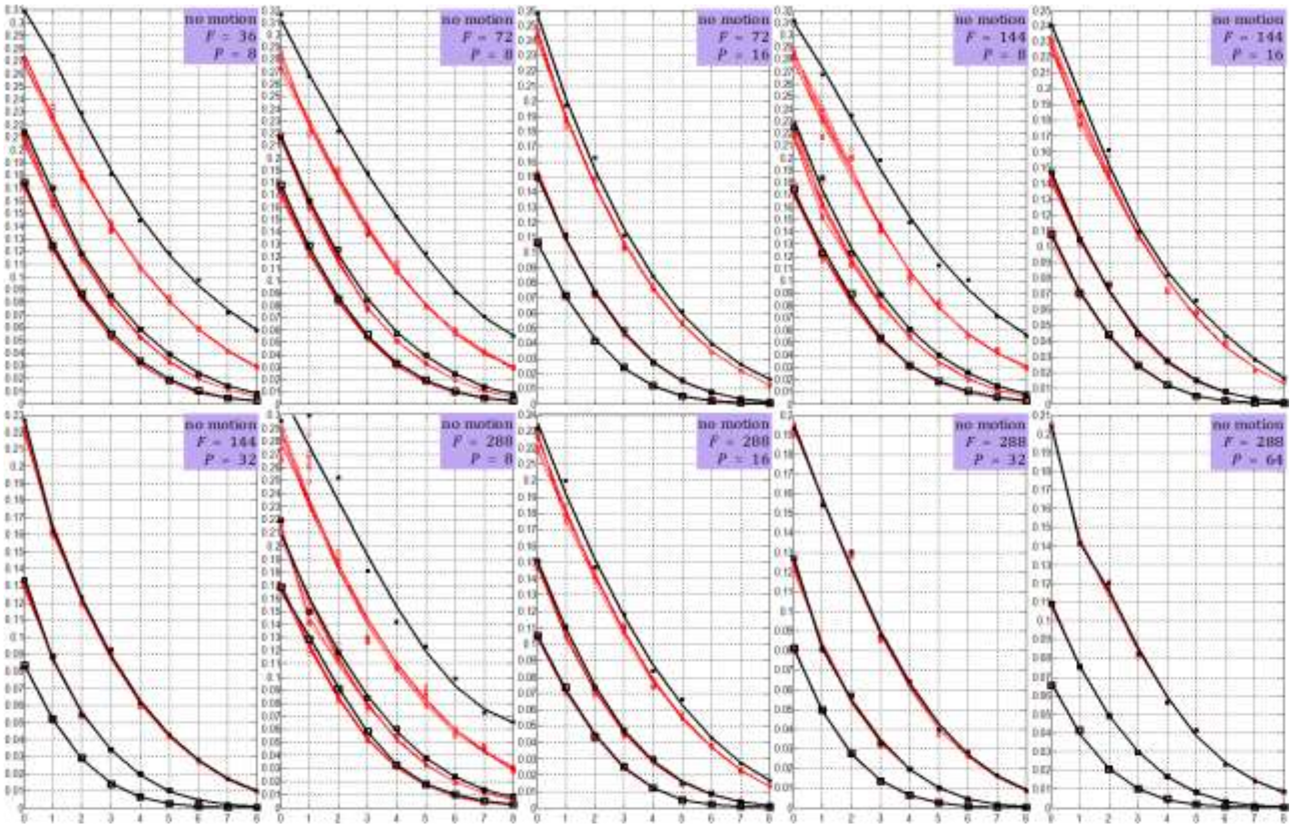

Figure 3 – BER performance versus BENDR by no motion

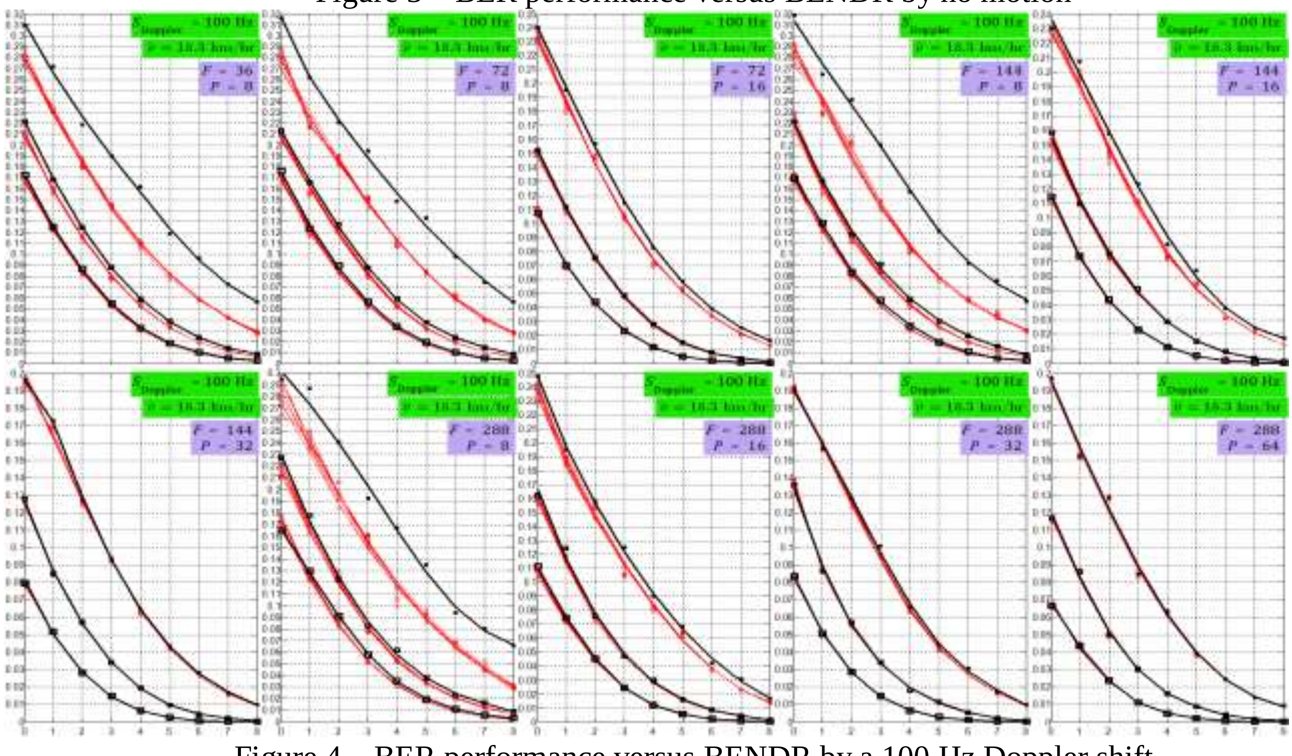

Figure 4 – BER performance versus BENDR by a 100 Hz Doppler shift

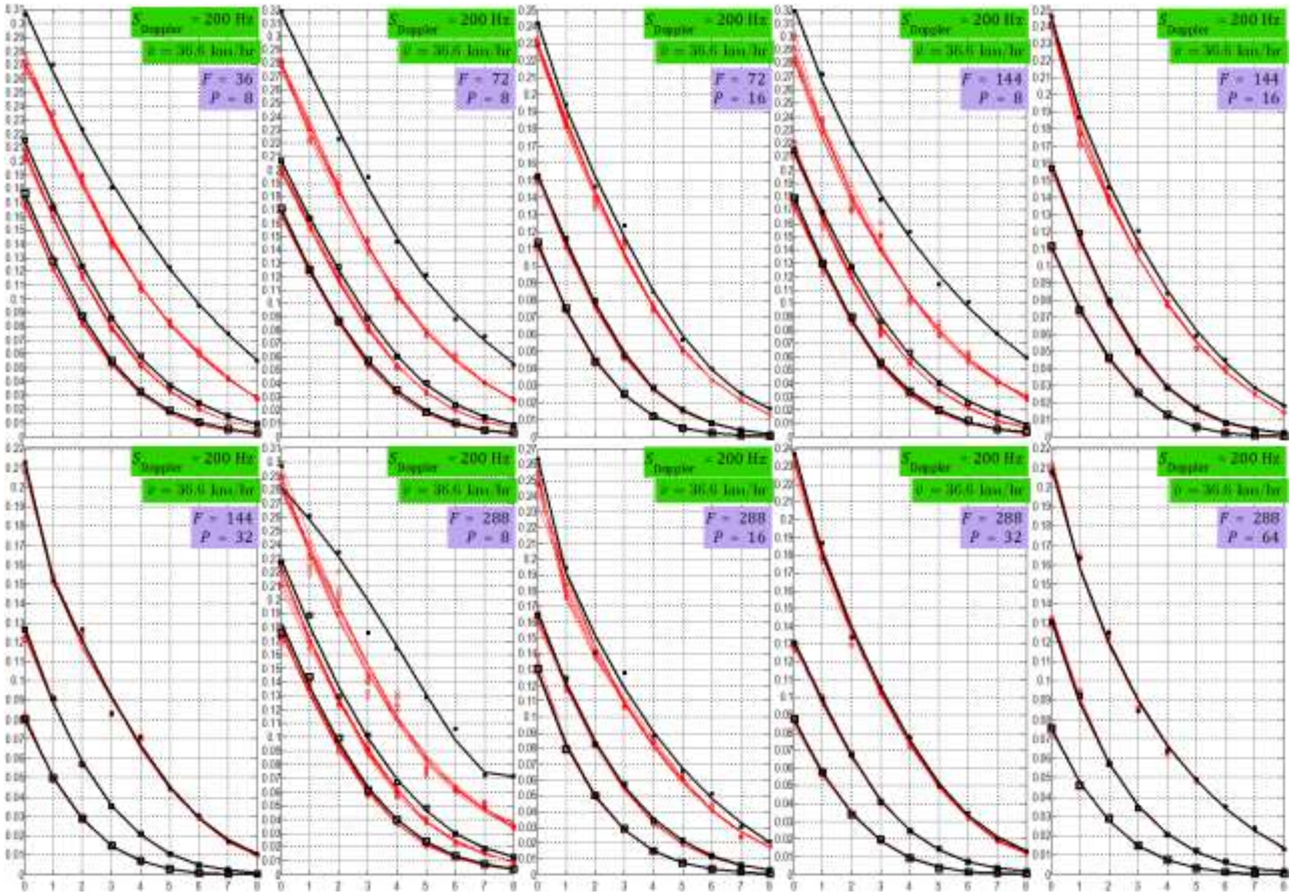

Figure 5 – BER performance versus BENDR by a 200 Hz Doppler shift

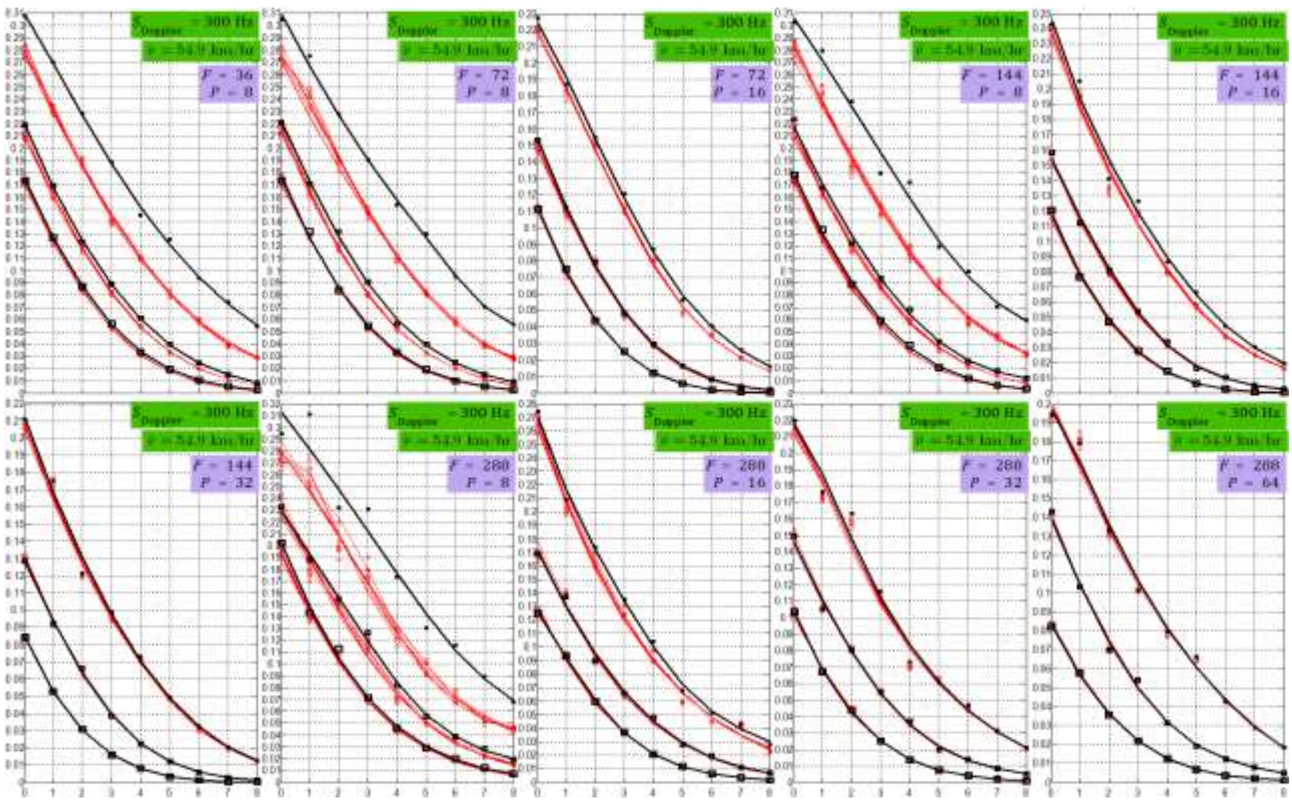

Figure 6 – BER performance versus BENDR by a 300 Hz Doppler shift (urban speeds)

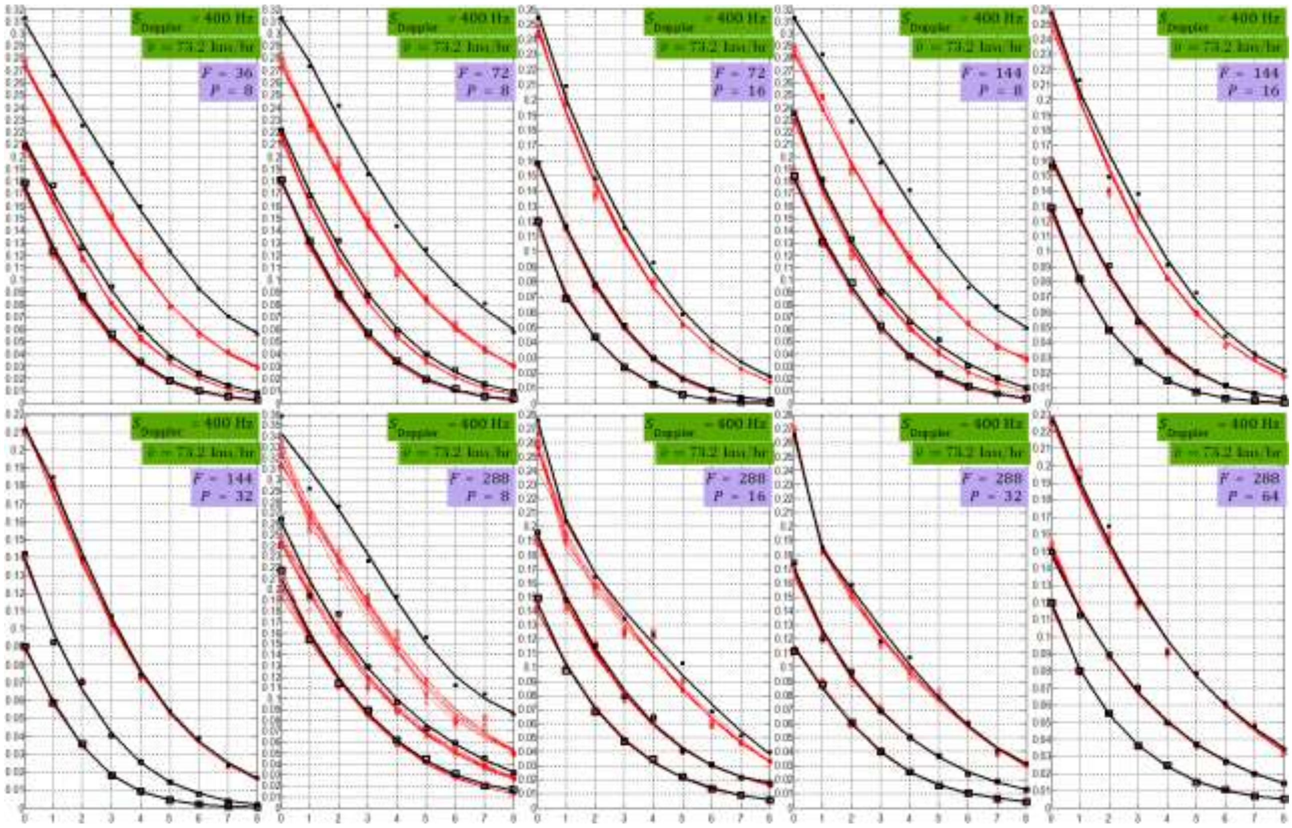

Figure 7 – BER performance versus BENDR by a 400 Hz Doppler shift (urban speeds).

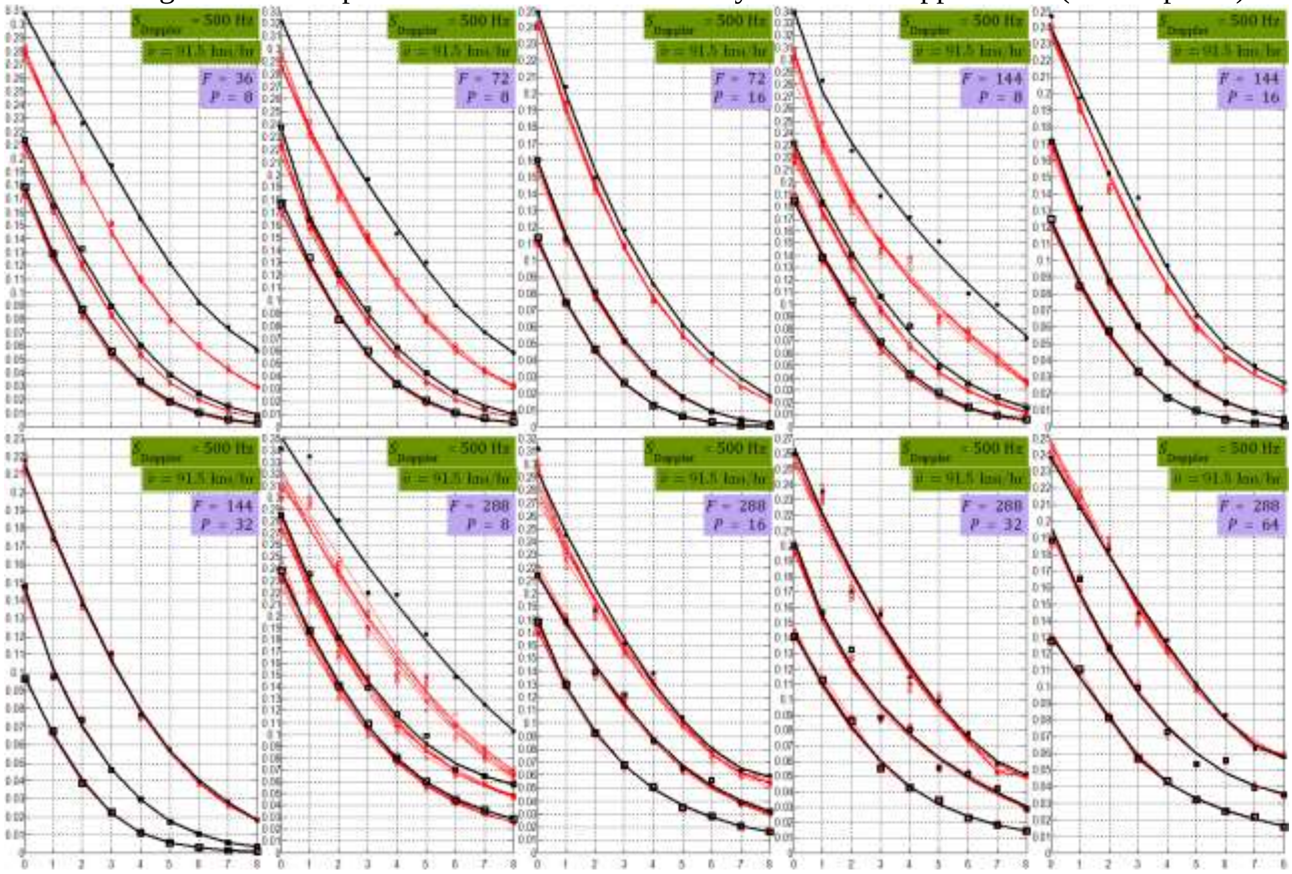

Figure 8 – BER performance versus BENDR by a 500 Hz Doppler shift (highway speeds)

Compared to no motion and slow-motion speeds, the worst BER performance deterioration at highway speeds is already seen in Fig. 8 for 4×4 MIMO systems transmitting longer packets with long pilot sequences. These are all subcases with $F = 288$. Thus, the BER at a BENDR of 0 dB of 4×4 MIMO, piloted with 64 symbols, by no motion is about 0.065 (Fig. 3), and it becomes about 0.13 by a 500 Hz Doppler shift (Fig. 8) by the same piloting. Therefore, the link quality of 4×4 MIMO systems at highway speeds (even not necessarily reaching 100 km/hr) may become twice as worse if the signal is weak. Meanwhile, the influence of the Doppler effect on 2×2 and 3×3 MIMO systems at such speeds is far less negative. Moreover, the MIMO systems transmitting the shortest packets (by the shortest pilot sequences), where $F = 36$ and $P = 8$, is almost not affected (for this, it is sufficient to compare the left upper corner subplot in Fig. 8 to that in Fig. 3). Furthermore, the MIMO systems with $F = 72$ and $P = 8$ are affected minimally.

It is worth noting that, as of highway speeds up to 100 km/hr (Fig. 8) and faster (Fig. 9), the polylines for the subcases of $F = 288$ by $P = 32$ and $P = 64$ are growing slightly disjoined (not stuck together as previously). However, the polylines for the subcase of $F = 144$ and $P = 32$ are still stuck together even at highway speeds reaching 128 km/hr (Fig. 10).

Another fact is that the topology of the polylines for the subcases of

$$\{F = 36, P = 8\},\ \{F = 72, P = 8\},\ \{F = 72, P = 16\} \tag{3}$$

and

$$\{F = 144, P = 8\},\ \{F = 144, P = 16\},\ \{F = 144, P = 32\} \tag{4}$$

remains roughly the same till the Doppler shift of 700 Hz corresponding to highway speeds reaching 128 km/hr (Fig. 10). This topology is summarized in Table 2, where an advantage of pilot sequences (by which the BER performance is better) is highlighted with dark color (the stronger advantage is highlighted with darker color). The tiny advantage is mentioned also.

Table 2 – The polylines topology (advantage of pilot sequences, if any) for subcases of (3) and (4) by no motion (Fig. 3) to highway speeds reaching 128 km/hr (Fig. 10)

	Pilot sequences by functions of		36	72	72	144	144	144
			8	8	16	8	16	32
2×2 MIMO	Walsh							
	Romanuke							tiny
3×3 MIMO	Walsh							
	Romanuke				tiny		tiny	
4×4 MIMO	Walsh							
	Romanuke		tiny	tiny		tiny	tiny	

At an 800 Hz Doppler shift (Fig. 11), the topology is starting to grow shattered for the subcase of $\{F = 144, P = 8\}$. Indeed, the polyline for the 2×2 MIMO Walsh pilot sequences does not resemble a smooth exponential decay (like it is at speeds not exceeding 100 km/hr), and the 2×2 MIMO Romanuke pilot sequences (from those eight orthogonal bases) appear disjoined. The polylines for MIMO systems transmitting longer packets (i. e. for all subcases with $F = 288$) are completely distorted. At such speeds close to express train speeds, it is impossible (and impracticable) to apply MIMO transmissions of long packets (even at high BENDR). Fig. 12 confirms this.

Nevertheless, the polylines topology in Table 2 remains almost the same even at really fast motion exceeding 180 km/hr (Fig. 13) and 200 km/hr (Fig. 14). The subcase of $F = 72$ and $P = 16$ at such express train speeds appears to be clearly the best: the BER is 0.235 to 0.255 for 2×2 MIMO, but it is 0.17 to 0.18 for 3×3 MIMO and it is 0.13 to 0.14 for 4×4 MIMO. This subcase is better than the subcase of $F = 144$ and $P = 32$, and the latter is outperformed by about 9 % to 18.5 %. Amazingly enough, at highway (100 km/hr and faster) and express train speeds (see Fig. 9 – 14), transmissions of very short packets become efficient at high BENDR.

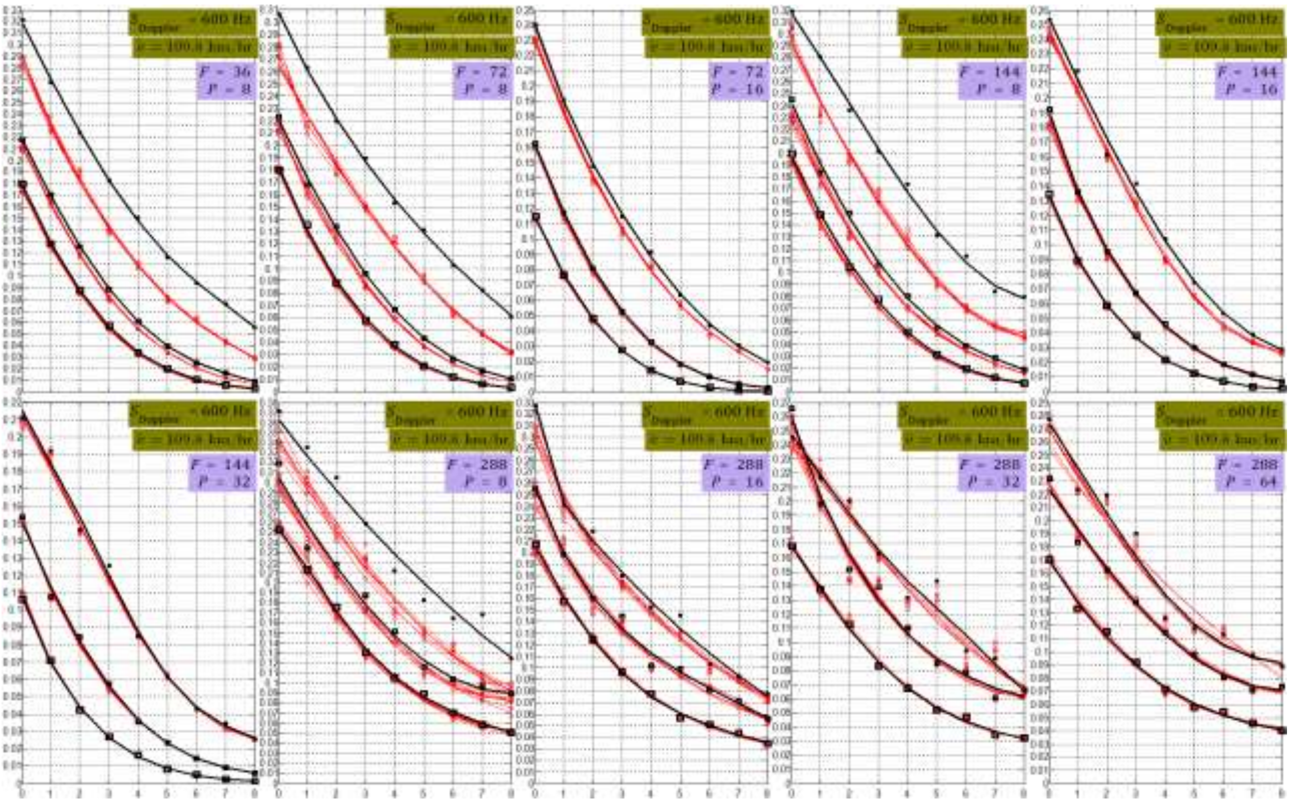

Figure 9 – BER performance versus BENDR by a 600 Hz Doppler shift (highway speeds)

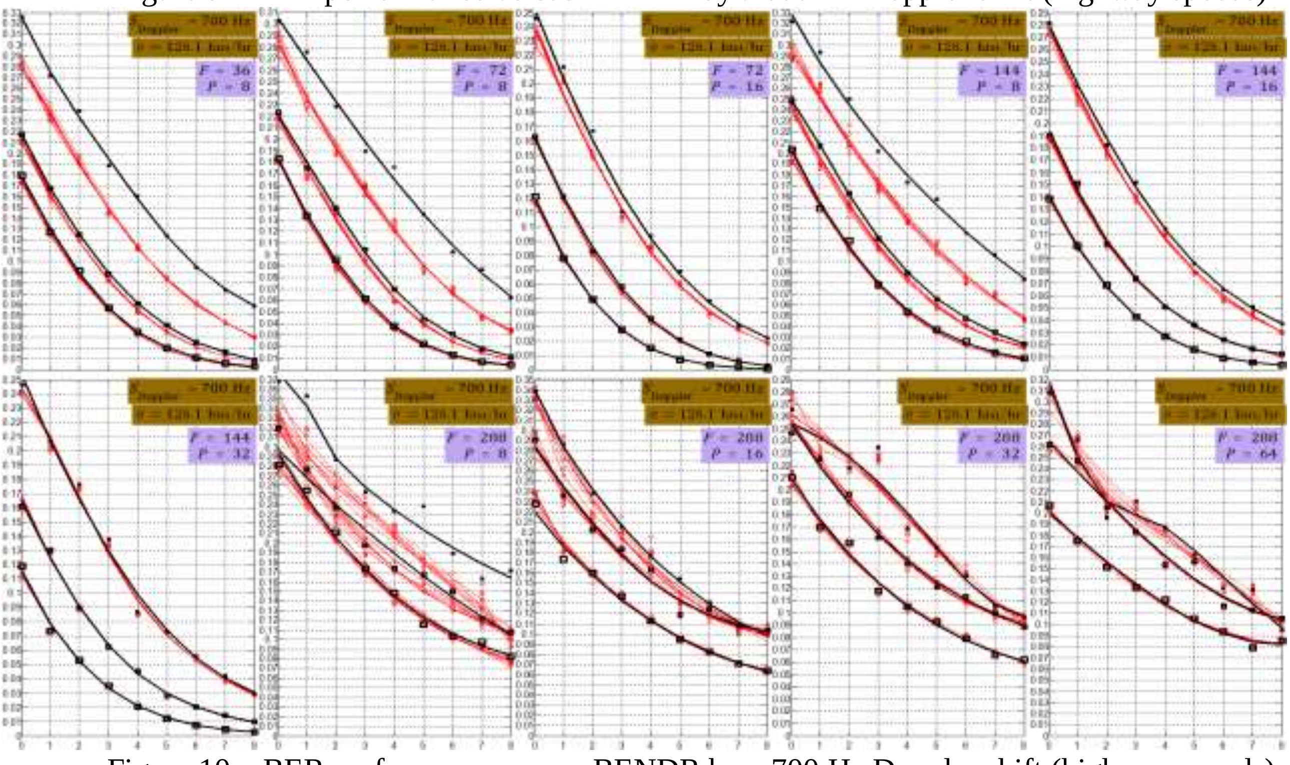

Figure 10 – BER performance versus BENDR by a 700 Hz Doppler shift (highway speeds)

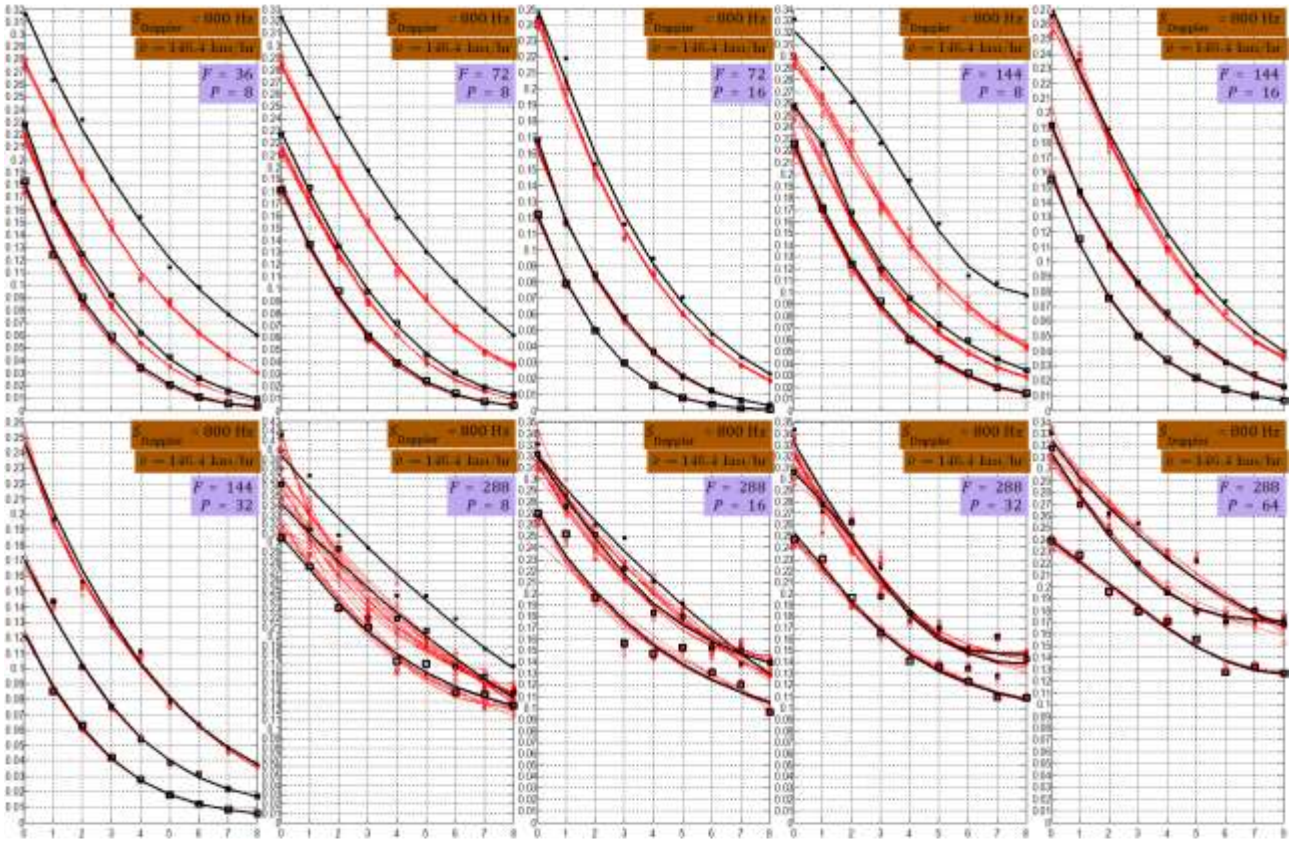

Figure 11 – BER performance versus BENDR by an 800 Hz Doppler shift (highway speeds)

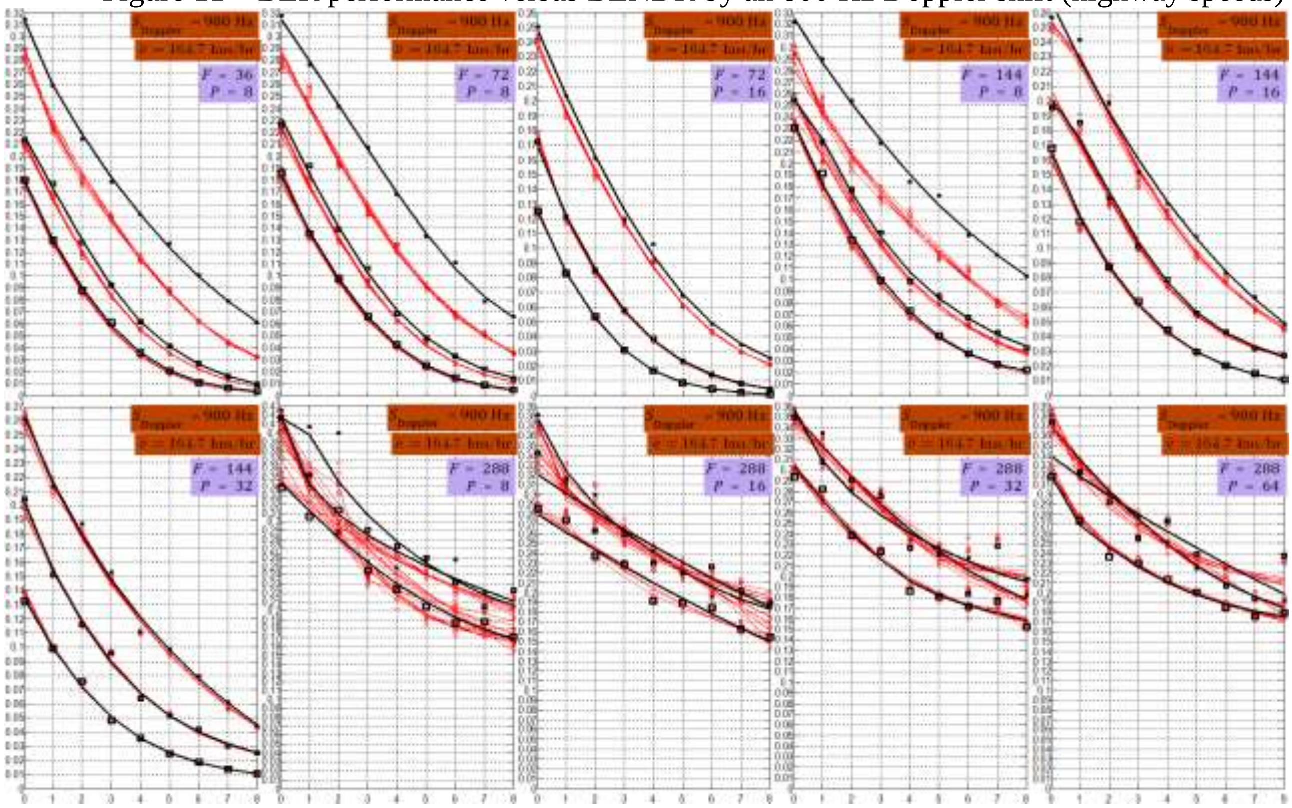

Figure 12 – BER performance versus BENDR by a 900 Hz Doppler shift (express train speeds)

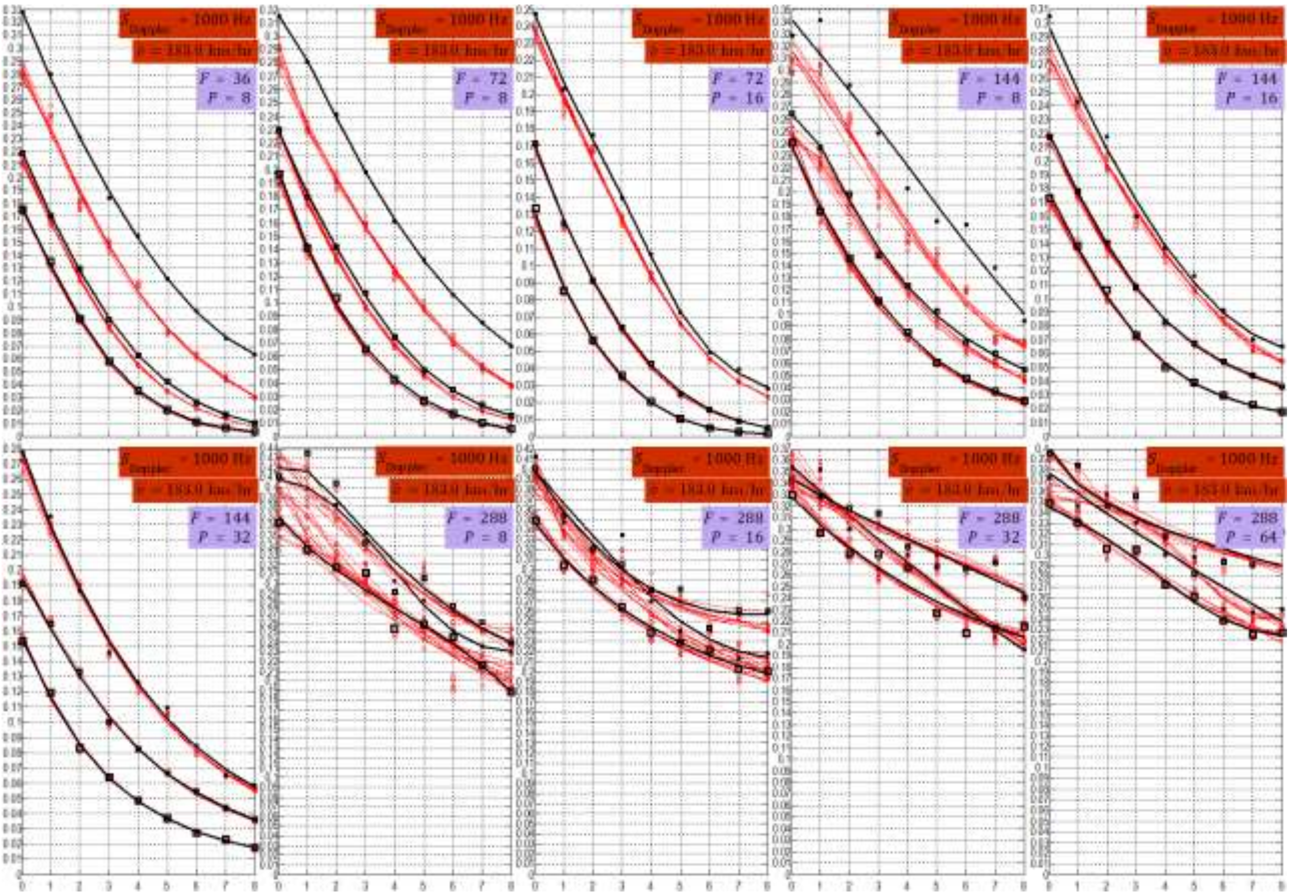

Figure 13 – BER performance versus BENDR by a 1000 Hz Doppler shift (express train speeds)

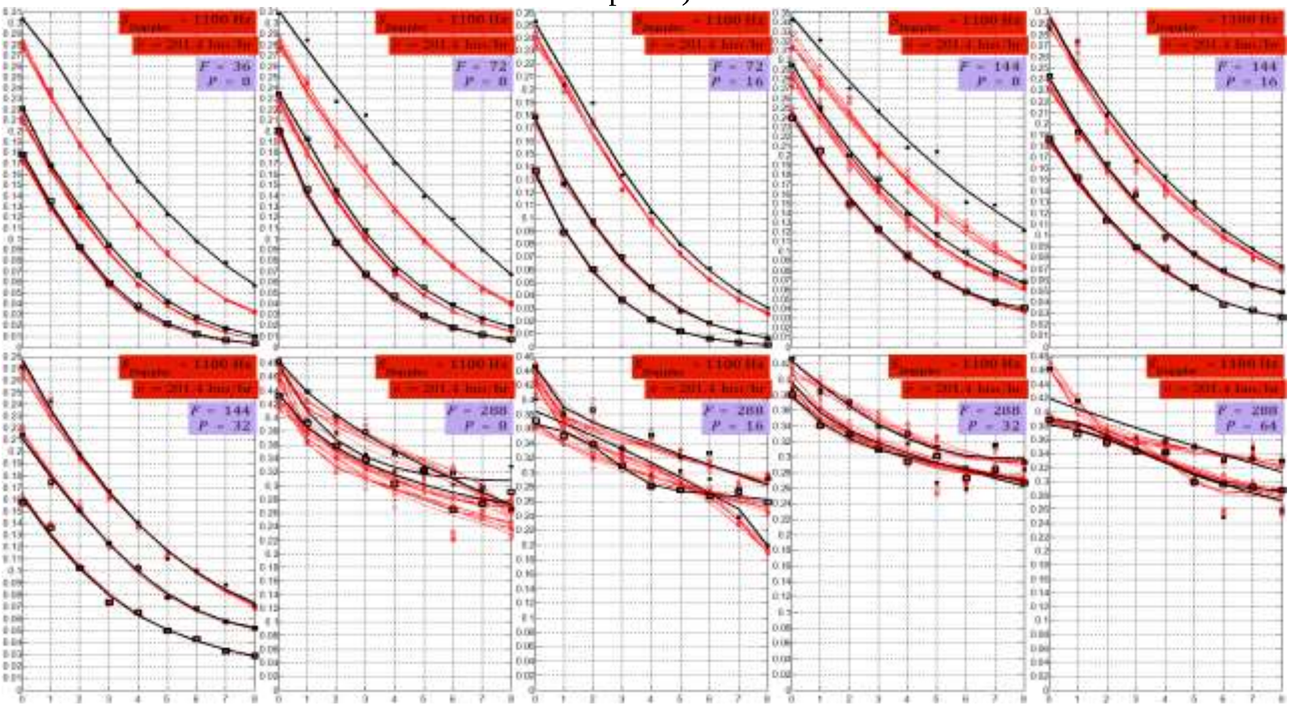

Figure 14 – BER performance versus BENDR by a 1100 Hz Doppler shift (express train speeds)

The averaged BER performance versus BENDR presented in Fig. 15 confirms that 2×2 MIMO Romanuke pilot sequences are significantly better than 2×2 MIMO Walsh pilot sequences, although it is impossible to determine the best basis of the binary functions. The average difference in the BER performance is about 7 to 15 %, but the difference decreases as the Doppler shift increases. Besides, 3×3 MIMO Romanuke pilot sequences outperform 3×3 MIMO Walsh pilot sequences also, where the difference is over 4.1 % by no motion and it decreases (the decrement is considered to be on average, it is not smooth, because some fluctuations occur due to small

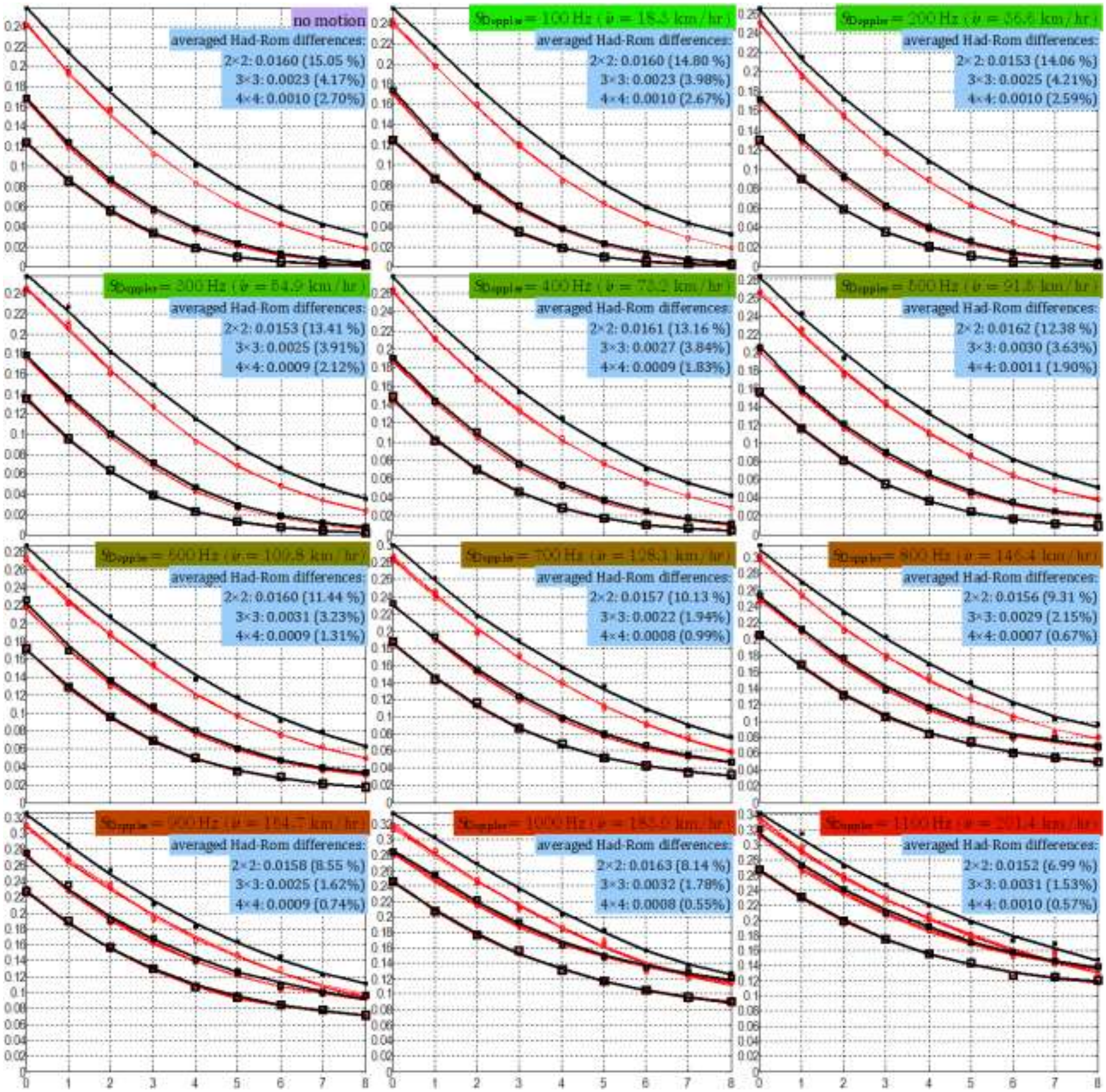

Figure 15 – The averaged BER performance versus BENDR

percentage) down to over 1.5 % at express train speeds exceeding 200 km/hr. Moreover, 4×4 MIMO Romanuke pilot sequences have lesser BER as well: the difference is about 2.7 % by no motion and it decreases (on average) down to over 0.5 % at express train speeds exceeding 200 km/hr.

Conclusions. In 2×2, 3×3 and 4×4 MIMO wireless communication systems with CSE by the OPSA, the Doppler effect negatively influences transmissions of long packets. At speeds exceeding 100 km/hr, it is impracticable to apply MIMO transmissions of long packets. In general, to maintain an appropriate MIMO link data rate, the packet length should be shortened as the motion speed increases. Moreover, the MIMO performance is substantially improved by increasing the number of antennas (not considering the case of long packets). Besides, under the de-orthogonalization caused by two negative-to-positive symbol errors, the Walsh pilot sequences are outperformed by MIMO Romanuke pilot sequences, so the latter are considered as an improvement of MIMO orthogonal sequences. However, the performance difference between the Romanuke and Walsh pilot sequences decays as a greater number of transmit-receive antenna pairs is used and the motion speed increases.

REFERENCES:

1. Berger L. T., Schwager A., Pagani P., Schneider D. M. MIMO Power Line Communications:

Narrow and Broadband Standards, EMC, and Advanced Processing. Devices, Circuits, and Systems. CRC Press, 2014.

2. Pätzold M. Mobile Fading Channels. Wiley, 2002.

3. Skolnik M. Introduction to Radar Systems. 3rd Ed. McGraw-Hill, New York, 2001.

4. Tsoulos G. MIMO System Technology for Wireless Communications. CRC Press, 2006.

5 .Lee W. C. Y. Mobile Communications Engineering: Theory and Applications. 2nd Ed. McGraw-Hill, 1998.

6. Stern H., Mahmoud S. Communication Systems. Pearson Prentice Hall, 2004.

7. Naguib A. F., Tarokh V., Seshadri N., Calderbank A. R. “Space-time codes for high data rate wireless communication: Mismatch analysis.” Proceedings of IEEE International Conference on Communications, Montréal, Québec, Canada, 8 – 12 June 1997, pp. 309 – 313.

8. Zhuang A., Lohan E. S., Renfors M. “Comparison of decision-directed and pilot-aided algorithms for complex channel tap estimation in downlink WCDMA systems.” Proceedings of 11th IEEE Personal and Indoor Mobile Radio Communications (PIMRC), Vol. 2, London, UK, September 2000, pp. 1121 – 1125.

9. Han H.-D., Nguyen D.-A., Nguyen V.-D., Nguyen T.-H., Zia M. “Pilot decontamination for multi-cell massive MIMO systems using asynchronous pilot design and data-aided channel estimation.” Physical Communication, vol. 30, 2018, pp. 76 – 85.

10. Walsh J. L. “A closed set of normal orthogonal functions.” American Journal of Mathematics, vol. 45, no. 1, 1923, pp. 5 – 24.

11. Romanuke V. V. Computational method of building orthogonal binary functions bases for multichannel communication systems with code channels division. Mathematical Modeling and Computational Methods. Ternopil State Technical University, Ternopil, Ukraine, 2006.

12. Tarokh V., Jafarkhami H., Calderbank A. R. “Space-time block codes from orthogonal designs.” IEEE Transactions on Information Theory, vol. 45, no. 5, 1999, pp. 1456 – 1467.

13. Romanuke V. V. “Generalization of the eight known orthonormal bases of binary functions to the eight orthonormal bases of binary surfaces.” Optoelectronic Information-Power Technologies, no. 2, 2007, pp. 263 – 271.

14. Romanuke V. V. “Simulation of code division by applying systems of orthogonal binary functions $\{\mathrm{wal}(w, \theta)\}_{w=0}^{L-1}$ and $\left\{\{\mathrm{rom}_u(r, \theta)\}_{r=0}^{L-1}\right\}_{u=1}^{8}$ in *L*-channeled CDMA-system.” Herald of Khmelnytskyi National University. Technical sciences, no. 6, 2008, pp. 121 – 132.

15. Torrieri D. Principles of Spread-Spectrum Communication Systems. 4th Ed. Springer, 2018.

16. Stuber G. L. Principles of Mobile Communication. 4th Ed. Springer, 2017.

17. Sklar B. “Rayleigh fading channels in mobile digital communication systems. Part 1: Characterization.” IEEE Communication Magazine, vol. 35, iss. 7, 1997, pp. 90 – 100.

18. Zheng L., Tse D. N. C. “Diversity and multiplexing: A fundamental tradeoff in multiple-antenna channels.” IEEE Transactions on Information Theory, vol. 49, iss. 5, 2003, pp. 1073 – 1096.

ЛІТЕРАТУРА:

1. Berger L. T. MIMO Power Line Communications: Narrow and Broadband Standards, EMC, and Advanced Processing. Devices, Circuits, and Systems / L. T. Berger, A. Schwager, P. Pagani, D. M. Schneider. – CRC Press, 2014.

2. Pätzold M. Mobile Fading Channels. – Wiley, 2002.

3. Skolnik M. Introduction to Radar Systems. 3rd Ed. – McGraw-Hill, New York, 2001.

4. Tsoulos G. MIMO System Technology for Wireless Communications. – CRC Press, 2006.

5. Lee W. C. Y. Mobile Communications Engineering: Theory and Applications. 2nd Ed. – McGraw-Hill, 1998.

6. Stern H. Communications System / H. Stern, S. Mahmoud. – Pearson Prentice Hall, 2004.

7. Naguib A. F. Space-time codes for high data rate wireless communication: Mismatch analysis / A. F. Naguib, V. Tarokh, N. Seshadri, A. R. Calderbank // Proceedings of IEEE International Conference on Communications, Montréal, Québec, Canada, 8 – 12 June 1997. – P. 309 – 313.

8. Zhuang A. Comparison of decision-directed and pilot-aided algorithms for complex channel tap estimation in downlink WCDMA systems / A. Zhuang, E. S. Lohan, M. Renfors // Proceedings of 11th IEEE Personal and Indoor Mobile Radio Communications (PIMRC), Vol. 2, London, UK, September 2000. – P. 1121 – 1125.

9. Han H.-D. Pilot decontamination for multi-cell massive MIMO systems using asynchronous pilot design and data-aided channel estimation / H.-D. Han, D.-A. Nguyen, V.-D. Nguyen, T.-H. Nguyen, M. Zia // Physical Communication. – 2018. – Vol. 30. – P. 76 – 85.

10. Walsh J. L. A closed set of normal orthogonal functions / J. L. Walsh // American Journal of Mathematics. – 1923. – Vol. 45, No. 1. – P. 5 – 24.

11. Romanuke V. V. Computational method of building orthogonal binary functions bases for multichannel communication systems with code channels division. – Mathematical Modeling and Computational Methods. – Ternopil State Technical University, Ternopil, Ukraine, 2006.

12. Tarokh V. Space-time block codes from orthogonal designs / V. Tarokh, H. Jafarkhami, A. R.

Calderbank // IEEE Transactions on Information Theory. – 1999. – Vol. 45, No. 5. – P. 1456 – 1467.

13. Romanuke V. V. Generalization of the eight known orthonormal bases of binary functions to the eight orthonormal bases of binary surfaces / V. V. Romanuke // Optoelectronic Information-Power Technologies. – 2007. – No. 2. – P. 263 – 271.

14. Romanuke V. V. Simulation of code division by applying systems of orthogonal binary functions $\{\mathrm{wal}(w, \theta)\}_{w=0}^{L-1}$ and $\left\{\{\mathrm{rom}_u(r, \theta)\}_{r=0}^{L-1}\right\}_{u=1}^{8}$ in *L*-channeled CDMA-system / V. V. Romanuke // Herald of Khmelnytskyi National University. Technical sciences. – 2008. – No. 6. – P. 121 – 132.

15. Torrieri D. Principles of Spread-Spectrum Communication Systems. 4th Ed. – Springer, 2018.

16. Stuber G. L. Principles of Mobile Communication. 4th Ed. – Springer, 2017.

17. Sklar B. Rayleigh fading channels in mobile digital communication systems. Part 1: Characterization / B. Sklar // IEEE Communication Magazine. – 1997. – Vol. 35, Iss. 7. – P. 90 – 100.

18. Zheng L. Diversity and multiplexing: A fundamental tradeoff in multiple-antenna channels / L. Zheng, D. N. C. Tse // IEEE Transactions on Information Theory. – 2003. – Vol. 49, Iss. 5. – P. 1073 – 1096.

DOI 10.33243/2518-7139-2020-1-2-50-64